Photonic fractional Fourier transformer with a single dispersive device

C. Cuadrado-Laborde,[1,2,3,*] A. Carrascosa,[1] A. Díez,[1] J. L. Cruz,[1] and M. V. Andres[1]

[1]*Departamento de Física Aplicada, ICMUV, Universidad de Valencia, Dr. Moliner 50, Burjassot E-46100, Spain*
[2]*CIOp (CONICET La Plata-CIC), P.O. Box 3, Gonnet 1897, Buenos Aires, Argentina*
[3]*Facultad de Ciencias Exactas e Ingeniería, Universidad Católica de La Plata, Buenos Aires, Argentina*
[*]*Christian.Cuadrado@uv.es*

Abstract: In this work we used the temporal analog of spatial Fresnel diffraction to design a temporal fractional Fourier transformer with a single dispersive device, in this way avoiding the use of quadratic phase modulators. We demonstrate that a single dispersive passive device inherently provides the fractional Fourier transform of an incident optical pulse. The relationships linking the fractional Fourier transform order and scaling factor with the dispersion parameters are derived. We first provide some numerical results in order to prove the validity of our proposal, using a fiber Bragg grating as the dispersive device. Next, we experimentally demonstrate the feasibility of this proposal by using a spool of a standard optical fiber as the dispersive device.

References and links

1. C. Cuadrado-Laborde and M. V. Andrés, "In-fiber all-optical fractional differentiator," Opt. Lett. **34**(6), 833–835 (2009).
2. C. Cuadrado-Laborde and M. V. Andrés, "Proposal and design of an all-optical in-fiber fractional integrator," Opt. Commun. **283**(24), 5012–5015 (2010).
3. C. Cuadrado-Laborde, "Proposal and design of a photonic in-fiber fractional Hilbert transformer," IEEE Photon. Technol. Lett. **22**(1), 33–35 (2010).
4. C. Cuadrado-Laborde, M. V. Andrés, and J. Lancis, "Self-referenced phase reconstruction proposal of GHz-bandwidth non-periodical optical pulses by in-fiber semi-differintegration," Opt. Commun. **284**(24), 5636–5640 (2011).
5. T. Alieva, M. J. Bastiaans, and M. L. Calvo, "Fractional transforms in optical information processing," EURASIP J. Appl. Sig. P. **10**, 1498–1519 (2005).
6. M. A. Muriel, J. Azaña, and A. Carballar, "Real-time Fourier transformer based on fiber gratings," Opt. Lett. **24**(1), 1–3 (1999).
7. J. Azaña, L. R. Chen, M. A. Muriel, and P. W. E. Smith, "Experimental demonstration of real-time Fourier transformation using linearly chirped fibre Bragg gratings," Electron. Lett. **35**(25), 2223–2224 (1999).
8. H. M. Ozaktas, Z. Zalevsky, and M. A. Kutay, *The Fractional Fourier Transform with Applications in Optics and Signal Processing* (Wiley, New York, 2001).
9. A. W. Lohmann, "Image rotation, Wigner rotation, and the fractional Fourier transform," J. Opt. Soc. Am. A **10**(10), 2181–2186 (1993).
10. W. Lohmann, Z. Zalevsky, R. G. Dorsch, and D. Mendlovic, "Experimental considerations and scaling property of the fractional Fourier transform," Opt. Commun. **146**(1-6), 55–61 (1998).
11. J. Hua, L. Liu, and G. Li, "Observing the fractional Fourier transform by free-space Fresnel diffraction," Appl. Opt. **36**(2), 512–513 (1997).
12. H. M. Ozaktas, S. Ö. Arık, and T. Coşkun, "Fundamental structure of Fresnel diffraction: natural sampling grid and the fractional Fourier transform," Opt. Lett. **36**(13), 2524–2526 (2011).
13. C. Cuadrado-Laborde, R. Duchowicz, R. Torroba, and E. E. Sicre, "Fractional Fourier transform dual random phase encoding of time-varying signals," Opt. Commun. **281**(17), 4321–4328 (2008).
14. A. W. Lohmann and D. Mendlovic, "Fractional Fourier transform: photonic implementation," Appl. Opt. **33**(32), 7661–7664 (1994).
15. C. Cuadrado-Laborde, P. Costanzo-Caso, R. Duchowicz, and E. E. Sicre, "Periodic pulse train conformation based on the temporal Radon-Wigner transform," Opt. Commun. **275**(1), 94–103 (2007).
16. K. Ennser, M. N. Zervas, and R. Laming, "Optimization of apodized linearly chirped fiber gratings for optical communications," IEEE J. Quantum Electron. **34**(5), 770–778 (1998).
17. B. H. Kolner, "Space-time duality and the theory of temporal imaging," IEEE J. Quantum Electron. **30**(8), 1951–1963 (1994).

1. Introduction

It is well known that the inherent speed limitations of conventional electronics can be overcome by all-optical circuits. Among them, it is necessary to study the possibility to perform all-optically different mathematical operations such as differentiation, integration, Fourier and Hilbert transforms, etc. The possible applications for these devices encompass optical pulse shaping, optical computing, information processing systems, and ultrahigh-speed coding, among other uses. Generally, the in-fiber way is preferred, because it offers simplicity, relatively low cost, low insertion loss, and inherent full compatibility with fiber-optic systems.

Recently, several all-optical in-fiber fractional operators have been proposed for fractional differentiation [1], fractional integration [2], and fractional Hilbert transformation [3]; together with some applications for these devices [4]. Fractional mathematical operators play an important role in information processing. In phase-space optics for example, the fractional Fourier transform (FrFT) has been proposed for phase retrieval, signal characterization, filtering, encryption, etc; see [5] and references therein. The fractionalization gives us a new degree of freedom (the fractional order) which can be used for more complete characterization of the temporal signal, in this way allowing a better control on the system.

It has been shown that a linearly chirped fiber Bragg grating (LCFBG) operating in reflection mode can be used to perform a Fourier transformation [6,7]. The principle of operation is based on the duality between Fresnel diffraction in space and dispersion in time of narrow-band pulses in dielectrics. It was shown that under a time-domain equivalence of the spatial Fraunhofer approximation, the device behaves as a Fourier transformer. In this work we extend that analogy designing an arbitrary-order photonic FrFT. This work is organized as follows. First we theoretically found the relationships linking the FrFT parameters with the dispersive parameters. Next, we numerically prove the validity of this proposal when a LCFBG is used as the dispersive device, together with a comparison with a standard FrFT implementation. Finally, we experimentally demonstrate the feasibility of this proposal obtaining the FrFT at different fractional orders on an input light pulse, by using different lengths of a standard optical fiber as a dispersive device.

2. Theory

The pth fractional Fourier transform of a temporal signal $f(t)$ will be denoted by $F_p[f(t)](t_p)$, whose mathematical definition, is given by [8,9]:

$$F_p\left[f(t)\right]\left(t_p\right) = c(p) \int_{-\infty}^{\infty} f(t) \exp\left[\frac{j\pi\left(t^2 + t_p^2\right)}{\varepsilon^2}\cot\left(\frac{p\pi}{2}\right)\right]\exp\left[-\frac{j2\pi t_p t}{\varepsilon^2}\csc\left(\frac{p\pi}{2}\right)\right]dt, \quad (1)$$

with $c(p) = \varepsilon \exp(-j\pi/4)[\csc(p\pi/2)]^{1/2}$; where p is the fractional-Fourier order, t_p is the variable in the fractional domain, and ε is an arbitrary fixed parameter with time dimension. We emphasize that the FrFT belongs to a two-parameter family of transformations, i.e. the fractional order p and the scaling parameter ε. In a FrFT, a change of the scaling parameter thoroughly changes the functional form of the output; as opposed to the ordinary Fourier transform, where only a scaling in the reciprocal variable is accomplished [10].

On the other hand, linear dispersive media can be modeled as linear time invariant systems by means of a transfer function. Let this transfer function $H(\omega)$ have flat amplitude and quadratic phase response (i.e., linear group delay) over a certain spectral bandwidth $\Delta\omega_H$:

$$H(\omega) = \exp\left[-j\Phi_{20}\omega^2/2\right], \quad (2)$$

where ω is the baseband angular frequency, and Φ_{20} is the first-order dispersion coefficient. Additionally, and only for simplicity, the average time delay has been ignored. Its impulse response −for complex envelopes of pulses with bandwidths narrower than $\Delta\omega_H$− will be given by:

$$h(t) = \exp\left[j\,t^2/2\Phi_{20}\right]. \tag{3}$$

The propagation of a single pulse in a linear dispersive regime can be expressed by convolving $f(t)$ with $h(t)$. Therefore, the output pulse $f_o(t)$ will be given by:

$$f_o(t') = \int_{-\infty}^{\infty} dt\; f(t) \exp\left[j(t'-t)^2/2\Phi_{20}\right]. \tag{4}$$

Intensities in Eqs. (1) and (4) can be made equal, provided:

$$\Phi_{20} = \left(\varepsilon^2/2\pi\right)\tan\left(p\pi/2\right), \qquad t_p \to t'\cos\left(p\pi/2\right). \tag{5}$$

Thus, the output of a linear dispersive system inherently provides a time-enlarged version in intensity of the FrFT. This result could be considered the time-domain counterpart of the existing equivalence between Fresnel diffraction and FrFT, which has been shown before for the spatial case [11,12]. Finally, a FrFT of pth order can be interpreted as a rotation in the time-frequency plane by $p\pi/2$, the details of this transformation can be found in Ref [13].

Now, let us review two important limiting cases: from negligible dispersion to strong dispersion. Let us assume also an input signal confined within a spectral bandwidth $\Delta\omega$ and time width Δt. When there is a negligible dispersion within the spectral bandwidth of the input signal, i.e.:

$$\Phi_{20}\Delta\omega^2 \ll 2\pi; \tag{6}$$

Equation (2) reduces to the unity. Therefore, the spectrum of the input signal remains unchanged, which is equivalent to no transformation at all, i.e., a FrFT of degree zero. On the contrary, in the high dispersion limit, i.e.:

$$\Delta t^2/\Phi_{20} \ll 2\pi, \tag{7}$$

the quadratic term in t can be neglected, see Eq. (4), reducing to an ordinary Fourier transform. Equation (7) is the time-domain equivalence of the Fraunhofer approximation. Hence, under the conditions given by Eq. (7), the output signal envelope is, within a phase factor, proportional to the Fourier transform of the input signal envelope evaluated at the angular frequency $\omega = t/\Phi_{20}$. Between the limits given by Eqs. (6) and (7), a continuum of FrFTs ranging from $p = 0$ to $p = 1$ can be achieved.

Equations (2) and (3) describe the propagation of temporal pulses, provided higher order dispersion terms are negligible within the input pulse`s bandwidth, including narrowband pulse propagation through an optical fiber. In that case:

$$\Phi_{20} = z\beta_{20}, \qquad D = -2\pi c\,\beta_{20}/\lambda^2, \tag{8}$$

where z is the fiber length, β_{20} represents the second-order derivative of the propagation constant respect to the angular frequency ω, and D is the dispersion parameter. Another solution widely used to provide enough dispersion is by using LCFBGs, because they can be designed with flat reflectivity and linear group delay within the operative bandwidth. Equation (3) also describes the impulse response of LCFBGs; so the reflection of a pulse from a LCFBG is mathematically identical to Fresnel diffraction.

Finally, and for comparison purposes, let us shortly review the standard way to perform a photonic FrFT. It consists in a tandem combination of three processes: quadratic phase modulation–dispersion–quadratic phase modulation [14,15]. Where the quadratic phase modulation factor ϕ_{20} and first-order dispersion factor Φ''_{20} are given by [15]:

$$\phi_{20} = \left(2\pi/\varepsilon^2\right)\tan\left(p\pi/4\right), \qquad \Phi''_{20} = \left(\varepsilon^2/2\pi\right)\sin\left(p\pi/2\right). \tag{9}$$

If we are only interested in the intensity of the FrFT, then the use of the final quadratic phase modulator can be avoided, since it is required for correcting the phase term of the FrFT. Nevertheless, one phase modulator is required when using this approach.

3. Numerical results

Our design is now tested by simulating the system response to a typical input pulse. In the simulations, it is assumed that the pulse is centered at the central frequency of a LCFBG. The proposed system consists of a single LCFBG incorporated into an optical circulator to operate in reflection mode. The spectrum of the output pulse is obtained just by multiplying the spectrum of the input pulse $F(\omega) = \Im[f(t)]$ by the complex grating spectral response $H(\omega)$. The output temporal waveform is then recovered by taking the inverse Fourier transform, i.e., $f_o(t) = \Im^{-1}[F(\omega)H(\omega)]$. Finally, since optical detection follows a square law, the detected waveform represents the FrFT of pth order of the input signal, i.e. $|f_o(t_p)|^2 = |F_p[f(t)](t_p)|^2$. In the following, we will design the LCFBG to work as a fractional Fourier transformer. Later, this design will be numerically tested by using a typical input signal.
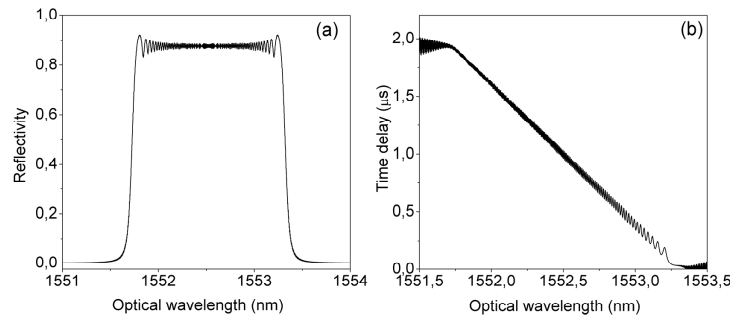

Fig. 1. (a) LCFBG reflectivity versus optical wavelength, the grating has a 200 GHz bandwidth centered at 1552.52 nm. (b) LCFBG reflection group delay; the grating provides a linear group delay with a slope (dispersion coefficient) of 1218 ps/nm.

The LCFBG response has been obtained by the simulation package *OptiGrating*. Regarding the design constraints of the LCFBG, the grating bandwidth determines the minimum time-width of the input pulses to be processed. Whereas, the LCFBG dispersion is determined by both the fractional order parameter p and desired scale factor ε, see Eq. (5). In this work, the LCFBG is designed to provide a dispersion coefficient of 1218 ps/nm over a 200 GHz bandwidth centered at the optical wavelength of 1552.52 nm. The device with this characteristic is 200 mm long and has a grating-period variation from 0.53496 μm to 0.53441 μm (unapodized uniform profile). By using transfer matrix theory and multilayer theory $H(\omega) = |H(\omega)|\exp[j\Psi(\omega)]$ is computed. Figures 1(a) and 1(b) show both the LCFBG reflectivity $|H(\omega)|^2$, and group delay $\tau_d = \partial\Psi/\partial\omega$, respectively. The first-order dispersion coefficient of the LCFBG Φ'_{20} can be obtained from $\Phi'_{20} = \partial\tau_d/\partial\omega = (\lambda_0^2/2\pi c)\partial\tau_d/\partial\lambda$, giving $\Phi'_{20} = 1.55 \times 10^{-21}$ s^2. It can be observed that the LCFBG provides the required features, and both the linearity of the group delay and the flatness of the reflectivity can be improved by an appropriate apodization of the grating`s refractive index perturbation [16]. Finally, the minimum grating length can be determined with $L = (c/2n_m)\Phi_{20}\Delta\omega_G$, where c is the speed of light in vacuum, n_m is the effective refractive index, $\Delta\omega_G$ is the grating operative optical bandwidth, and Φ_{20} is given by Eq. (5). Of course, the spectral bandwidth of the input signal $\Delta\omega$ should be lower than $\Delta\omega_G$.

From a rapid inspection of Eq. (5) becomes clear that multiple combinations between FrFT's orders p and scale factors ε are available when the dispersion is fixed to a given value −in our case $\Phi'_{20} = 1.55 \times 10^{-21}$ s^2−; from these, we select $p = 0.35$ and $\varepsilon^2 = (1/2\pi) \times 10^{-19}$ s^2. Figure 2(b) shows the mathematically obtained 0.35th order FrFT, of the input signal shown in Fig. 2(a), which consists of a twin optical pulse of 6 ps (FWHM) each separated by 50 ps.

Figure 2(c) shows the simulated reflected pulse in the LCFBG. By comparing Figs. 2(b) and 2(c) we conclude that they are identical, except by the scaling in the time domain, which can be easily corrected according to the time scaling of Eq. (5). Figure 2(d) shows both signals, i.e. the mathematically obtained FrFT and the reflected pulse in the LCFBG after applying Eq. (5) in the later for time-scale correction. It can be observed that both signals superimpose upon the other, indicating the close resemblance between them. The average time delay that the reflected signal in the LCFBG undergoes because of the group delay effect has been corrected in Fig. 2.
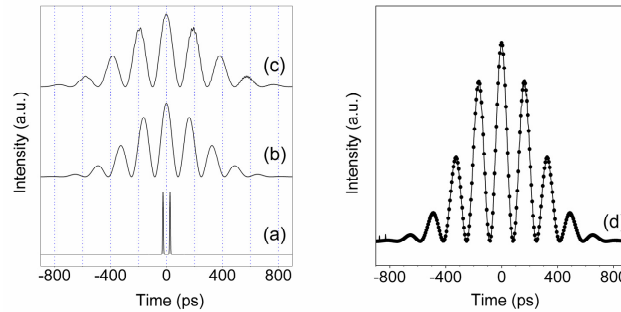

Fig. 2. (a) Input signal consisting in a twin Gaussian optical pulse of 6 ps each (FWHM) separated by 50 ps. (b) Mathematically obtained 0.35th order FrFT with scale factor $\varepsilon^2 = (1/2\pi) \times 10^{-19}$ s^2. (c) Simulated response after reflection in the LCFBG shown in Fig. 1 of the input pulse shown in (a). (d) The same signals shown in (b) and (c) are represented together for comparison purposes, except that now the signal shown in (c) has a time-scaling correction.

It is worth to compare this proposal with a standard photonic FrFT implementation [14,15]. In the later, it would be necessary at least one phase modulator with quadratic phase modulation factor of $\phi_{20} = 1.11 \times 10^{20}$ rad × Hz^2; plus a LCFBG with a first-order dispersion coefficient of $\Phi''_{20} = 1.32 \times 10^{-21}$ s^2, see Eq. (9). Usually quadratic-phase modulation is achieved by driving an electro-optic modulator with an electrical sinusoidal signal at the modulation frequency ω_m −being $\phi_{20} \propto \omega_m^2-$; which is only approximately quadratic at a cusp of the sinusoid. Therefore, the optical input signal must be restricted to a usable time aperture T_a centered on a cusp. Thus, by limiting the influence of higher order (fourth) phase terms to a 2%, results in $T_a \approx \phi_{20}^{-1/2}$ [17]. Thus, the proposed setup in this work is considerably simpler since phase modulators are not necessary.

4. Experimental results

Now, as a proof of concept, we experimentally demonstrate the feasibility of this proposal by obtaining all-optically the FrFT at different fractional orders on an input light pulse, by using different lengths of a standard optical fiber as a dispersive device. The input light pulses were provided by a passively mode-locked ytterbium fiber laser (emission wavelength of 1038 nm), which can be satisfactory adjusted with a hyperbolic secant profile. By previous measurements we also determined that the light pulses provided by this laser are linearly chirped with $C = -11$. In this way the input light pulse were modeled by $f(t) = \mathrm{sech}(t/T_0)\exp(-jCt^2/2T_0^2)$, with $T_0 = 12$ ps, which corresponds to a FWHM of 21 ps. The light pulses were detected with a 50 GHz bandwidth sampling oscilloscope. The dispersion line was made with a commercially available optical fiber (SM980, low numerical aperture Fibercore), with a measured first order dispersion $D = -44$ ps/nm × Km at the lasing wavelength. Three different fiber lengths were used: 101 m, 214 m, and 315 m; by using Eq. (8), this results in the following first-order dispersion coefficients $\Phi_{20} = 2.54$ ps^2, 5.4 ps^2, and 7.94 ps^2, respectively. Finally, by using Eq. (5) and by selecting $\varepsilon^2 = 500$ ps^2, we obtain the following fractional orders $p = 0.0203, 0.043$, and 0.063, for each fiber length, respectively.

The experimental setup is shown in Fig. 3(a). Figure 3(b) shows the experimentally detected input pulse together with its corresponding fitting by a hyperbolic secant profile. In

the same figure, it is shown the mathematically obtained FrFT (scale factor $\varepsilon^2 = 500$ ps^2) of the hyperbolic secant profile shown in Fig. 3(b), for $p = 0.0203$ [Fig. 3(c)], $p = 0.043$ [Fig. 3(d)], and $p = 0.063$ [Fig. 3(e)]. For each theoretically obtained FrFT, it is also shown the experimentally detected output light pulse after propagating by a fiber length of 101 m, 214 m, and 315 m, respectively. The time scale of the propagated pulse was modified according to Eq. (5), with the corresponding fractional order. There is a good degree of resemblance between analytically obtained and experimentally detected FrFT. There is also a deviation that increases with the fractional order in the trailing edge, but this could be motivated by the fact that the proposed input profile does not fit the experimental data perfectly.
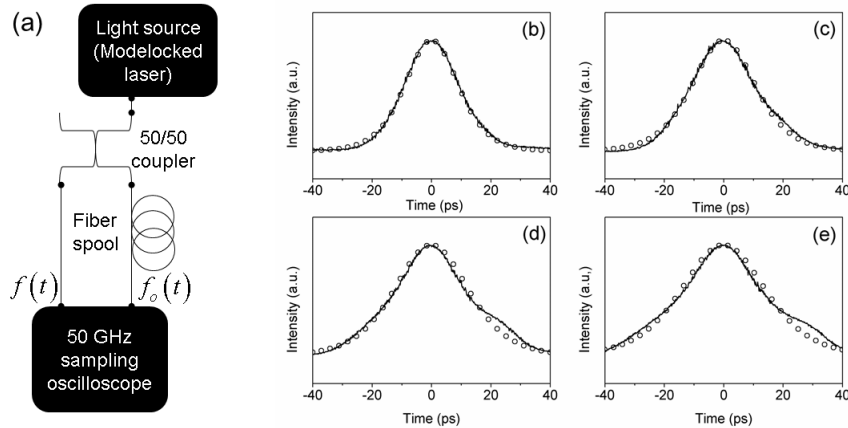

Fig. 3. (a) Scheme of the experimental setup. (b) Input pulse provided by the modelocked laser (solid curve), and its corresponding fitting by a sech profile (scatter points). (c) Mathematically obtained 0.0203th order FrFT of the sech profile shown in (b), and experimentally detected output light pulse after propagation in a fiber length of 101 m. (d)-(e) Same as in (c) but for 0.043th and 0.063th order FrFTs and propagations of 214 m and 315 m, respectively.

5. Conclusions

In this work we used the temporal analog of spatial Fresnel diffraction to design a temporal fractional Fourier transformer with a single dispersive device, in this way avoiding the use of quadratic phase modulators. The proposal is based in the use of a single dispersive passive device. The relationships linking the fractional Fourier transform order and scaling factor with the dispersive parameter were found. We first provide some numerical results in order to prove the validity of this proposal when a fiber Bragg grating is used as a dispersive device. Next, we experimentally demonstrate the feasibility of this proposal by obtaining all-optically the FrFT at three different fractional orders on an input light pulse provided by a modelocked laser. In this case we use different lengths of a standard optical fiber as a dispersive device.